Journal of Petroleum Science and Technology 14(3): 43, 2024, Pages 18-29
DOI:10.22078/jpst.2025.5506.1944

Journal of Petroleum Science and Technology
Research Paper
https://jpst.ripi.ir/

Formation Evaluation and Reservoir Quality Assessment of the AN-field Offshore Douala/Kribi Campo Basin, Cameroon

Ndip Edwin Ayuk[1*], Batembe Joseph Valery[1] and Josephine Kawa Maximus[2]
1. Department of Geology, University of Buea, Cameroon
2. Department of Petroleum and Geological Engineering, University of Guyana, Turkeyen Campus, Georgetown, Guyana

Abstract
The AN field, located offshore in the Douala Sub-Basin within the Douala/Kribi-Campo Basin, is part of the larger Aptian Salt Basin in Equatorial West Africa. This study focuses on evaluating the petrophysical properties and determining the reservoir quality of the sandstones in the AN Field to enhance production efficiency. Furthermore, well log data, including caliper, gamma-ray, density, neutron, sonic, and resistivity logs, were collected from Well 1 and Well 2 (pseudonym) in the AN field Douala Basin and analyzed using Techlog version 2015.1 software for petrophysical analysis and reservoir quality assessment. Moreover, the lithologic sequence consists of sandstone beds alternating with shale. In addition, three sandy reservoir units were identified (R1, R2, and R3), with thicknesses ranging from 16.6 to 53.8 m, identified in Wells 1 and 2. In addition, the reservoirs exhibited poor average formation porosity (1.54 - 16.53%), low average permeability (0.02 - 5.93 mD), and significantly high average water saturation (64.81-99.1%). In addition, analysis of true formation resistivity values versus water saturation indicated that all reservoir units in both wells were water saturated and unable to yield a commercial quantity of hydrocarbons. Furthermore, the gamma-ray log patterns indicate the depositional environment to be a deep marine setting, specifically fan valley sediments, encompassing braided river floodplains, deep tidal channel fills, and submarine fan lobes. In addition, the identified depositional environment aligns with a deep marine setting, which emphasizes the need for further exploration and assessment to optimize production efficiency in this area. Moreover, the results from this study will guide wellsite decisions, reservoir development, and production planning, and impact critical financial decisions at every stage of the Exploration and Production lifecycle in the Douala Sub-Basin, Cameroon.

Keywords: Douala Sub-Basin, Petrophysical Analysis, Reservoir Quality Assessment, Sandstones.

Introduction
The process of assessing hydrocarbon reservoirs through formation evaluation is vital, as it involves a comprehensive blend of geology, petrophysics, and reservoir engineering to achieve a thorough reservoir characterization [1-3]. In addition, well logs are the primary means employed to delineate petrophysical properties like lithology, porosity, saturation, and permeability [4-6]. Understanding these petrophysical characteristics is imperative for evaluating the quality and production potential of oil and gas reservoirs [7-9]. Moreover, a detailed evaluation of the petrophysical properties of reservoir rocks enhances the capacity to estimate hydrocarbon reserves, determine reservoir bed thickness, and differentiate between gas, oil, and water-bearing strata by examining their electrical resistivity and relative permeability values [10-13].
The Douala/Kribi-Campo basin, found along the southwestern coast of Cameroon, forms the northern segment of the Aptian Salt Basin located in Equatorial West Africa [14,15]. In addition, this basin extends southwards to Namibia and is situated within the Gulf of Guinea, bordered by the oil-rich regions of Angola, Congo, Gabon, and Equatorial Guinea to the south, as well as the Niger/Rio del Rey Basin to the north [14]. Moreover, this basin is renowned for its bowl-like configuration, significant detrital debris content, and various geological formations shaped by tectonic activities [16,17]. In addition, hydrocarbon production commenced in the offshore Douala Basin as early as 1977, with a rapid decline from 180,000 barrels per day (bpd) in 1985 to approximately 60,000 bpd, prompting the quest for fresh reserves [18]. Furthermore, the relevance of petroleum in bolstering the economic well-being of both developed and developing nations cannot be overstated due to its multifaceted applications. Moreover, continuous efforts are underway to explore and unearth new deposits to sustain these benefits. Also,

*Corresponding author: Ndip Edwin Ayuk, *Department of Geology, University of Buea, Cameroon*
E-mail addresses: ndip.ayuk@ubuea.cm
Received 2024-07-16, Received in revised form 2024-10-03, Accepted 2025-04-15, Available online 2025-08-16

innovations are indispensable to enhancing current production methods and locating untapped fields.

Numerous studies have explored the geological characteristics of the Douala Basin's onshore region over the years. Moreover, fieldwork investigations conducted by 19 and 20, as well as sedimentological examinations by 21 and paleontological analyses by 22 have contributed significantly to our understanding. However, there is a noticeable gap in research focusing on the offshore sector. In addition, recent studies in the offshore portion of the basin have honed in on deep-water channel systems, underscoring the importance of comprehending channel morphology for compelling hydrocarbon exploration in deeper waters [23, 24].

The offshore reservoirs in the Douala Basin exhibit promising petrophysical properties, boasting porosity levels ranging from 20 to 30.8%, substantial hydrocarbon saturation, and favorable permeability, particularly in channel sands, submarine fan lobe sands, and deep tidal channel-fill [23, 25]. The AN Field is located offshore in the Douala Sub-Basin, a component of the broader Douala/Kribi-Campo (DKC) Basin (Fig. 1). Due to a confidentiality agreement with Cameroon's National Hydrocarbon Corporation (SNH), the precise well locations remain undisclosed. This study aims to improve the understanding of reservoir characteristics within the AN Field by utilizing subsurface data to reassess its hydrocarbon potential. Specifically, it focuses on the petrophysical characterization of the reservoirs using well log data, with key objectives including the identification of lithologic sequences, delineation of major reservoir units, evaluation of their petrophysical properties, and determination of the depositional environment. Ultimately, the study seeks to reduce uncertainties associated with hydrocarbon exploration and production in the area.

Geological Settings

The Regional Geologic Settings and Stratigraphy of Douala / Kribi Campo Basin

The Douala/Kribi-Campo basin is part of a series of continental shelf basins stretching across West Africa from the Niger Delta in Cameroon to the Walvis Ridge near the Angola-Namibia border. Moreover, it is subdivided into two sections: the Kribi-Campo sub-basin to the south and the Douala sub-basin to the north. Furthermore, the Douala sub-basin extends between latitudes 3˚03'N and 4˚06'N, and longitudes 9˚00'E and 10˚00'E, covering an area of 12,805 km^2 (Fig. 2). This sub-basin has a crescent shape, starting from the southeastern border of Mount Cameroon with an onshore width of about 70 km, gradually narrowing towards the South up to Londji. Furthermore, the eastern boundary of the sub-basin is formed by the late Proterozoic Pan-African belt. Moreover, the formation of the Douala sub-basin and its half-graben structure is attributed to an E-W distension event that led to the separation of the African and South American continents, resulting in the opening of the South Atlantic [27].

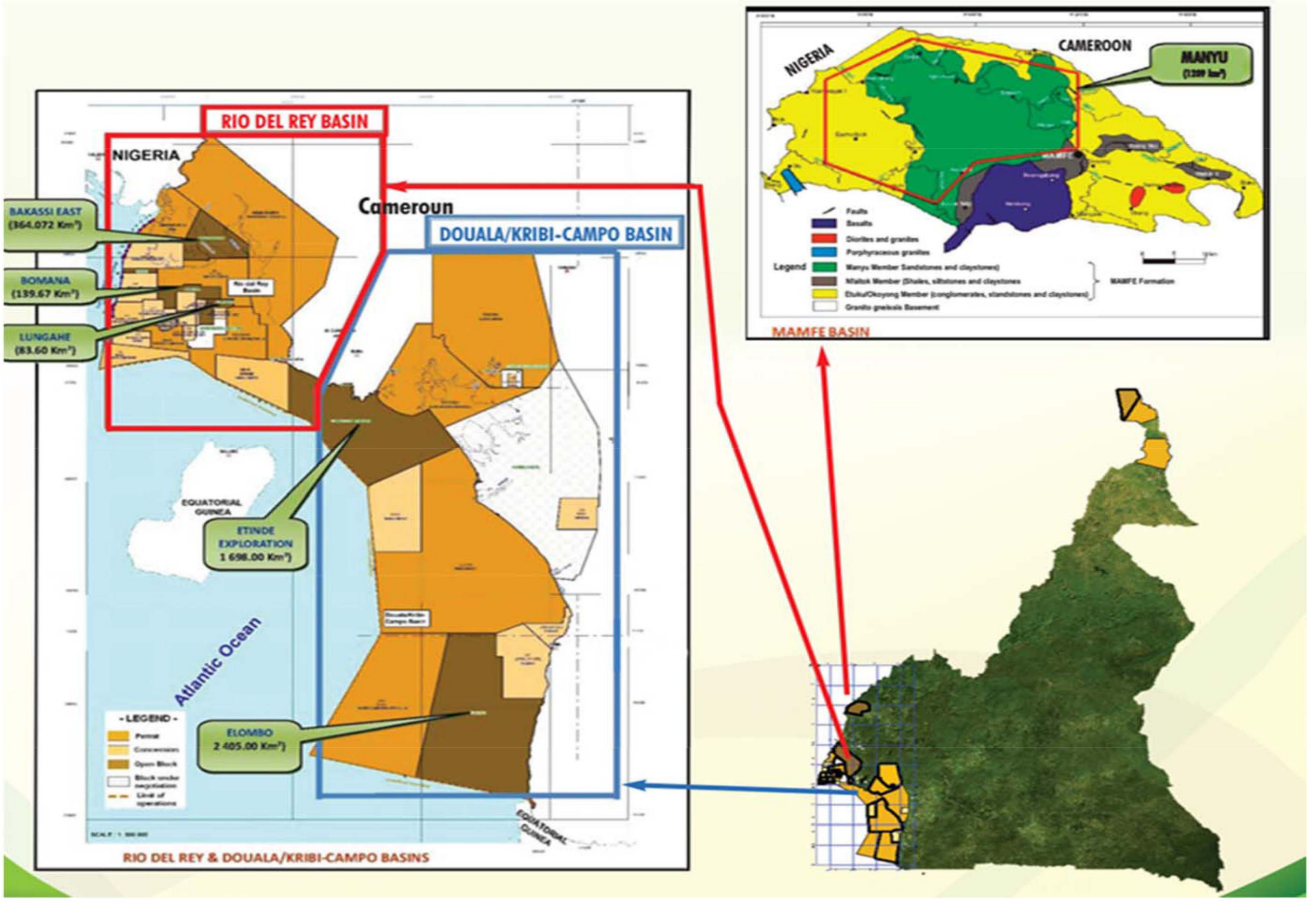

Fig. 1 Map showing Cameroon (a), the Douala /Kribi Campo Basin and Rio Del Rey Oil block with AN Field in red triangle (B) and (C) Mamfe basin [26].

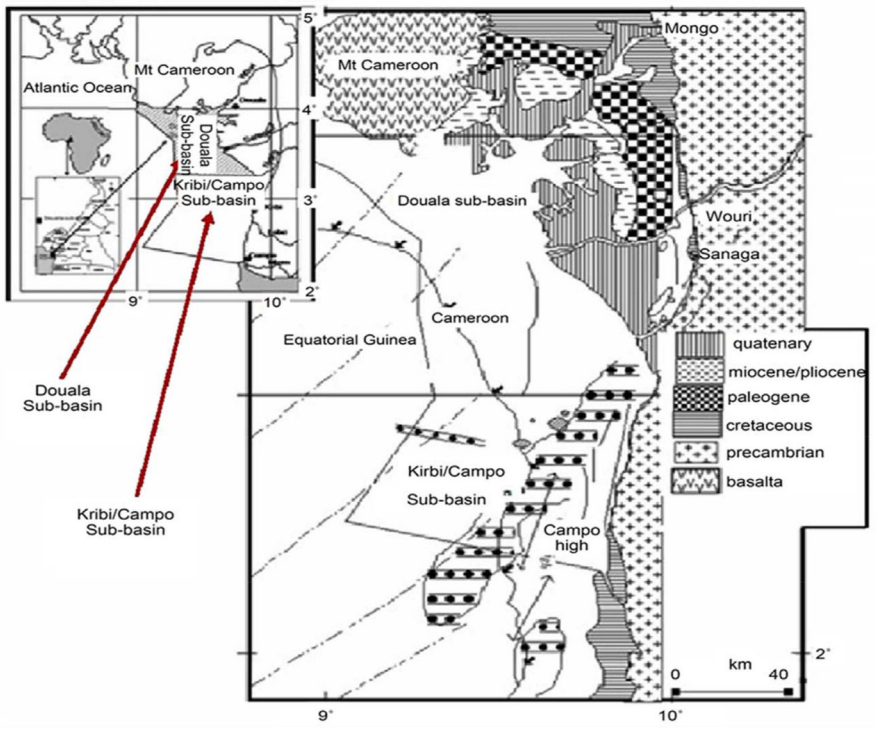

Fig. 2 Location map of Cameroon (West Africa) and outlines of the Douala and Kribi/Campo sedimentary sub-basins. (Modified from 27 & 30).

On the other hand, the Kribi-Campo sub-basin, located onshore and offshore Cameroon, falls within latitudes 2˚20'N - 3˚20'N and longitudes 9˚15'E - 10˚00'E, covering approximately 6195 km^2. The subsurface of this basin is primarily composed of Archean rocks of the Ntem complex overlain by Paleoproterozoic rocks of the Nyong Unit. The northern region consists of Precambrian rocks affected by the Pan-African episode, comprising mostly schists and gneisses intruded by granites and diorites. In contrast, the southern part is characterized by the Ntem complex, representing the northern edge of the Congo craton, with granulite facies rocks formed during the Archean and reactivated during the Eburnean orogeny. Furthermore, the coastal region of the basin is dominated by Cretaceous sediments, predominantly sandstones with minor occurrences of limestone and shales. The geological evolution of these basins has resulted in a variation of sedimentary environments along the West African coast over time [25-29].

Stratigraphy of Douala /Kribi Campo Basin

The lithostratigraphy of the Douala Sub-Basin includes seven major formations that are connected to its geodynamic and sedimentary evolution [31]. Moreover, the formations consist of various layers, starting from the Precambrian Basement, followed by the Mundeck Formation, the Logbaba Formation, the N'kapa Formation, the Souellaba Formation, the Kribi Formation, the Matanda Formation, and finally, the Wouri Formation (Fig.3). Each Formation has distinct characteristics and compositions, ranging from ancient Precambrian rocks in the basement to more recent sediments like sands, shale, sandstone, and mudstones in the upper formations. Moreover, the sedimentary cycles within these formations reveal different environments such as continental, marine, and deltaic, with unique depositional patterns and rock types that offer valuable insights into the geological history of the Douala Basin.

Materials and Methods

This research employed datasets provided by the National Hydrocarbon Corporation of Cameroon, specifically wireline logs in LAS format. These logs were utilized to calculate key petrophysical parameters and to interpret the depositional environment of the reservoir. Additionally, the data supported the evaluation of reservoir continuity and the spatial distribution of petrophysical properties. Collectively, these insights contribute to a more comprehensive understanding of the reservoir, thereby enhancing its overall characterization within the study area. Well 1 and Well 2 in the AN field were the focus of the study, with the data meticulously organized, sorted, and quality checked before being imported into Techlog software for visualization as log Curves. The software was employed for data quality control, interpretation, and analysis of the digitized wireline logs. Petrophysical assessment was categorized into qualitative and quantitative evaluations. Furthermore, the Gamma ray (GR) log signature was used to delineate the various lithological units in each of the studied wells, whereby the sand bodies were differentiated from the shale bodies. In addition, the sand bodies were identified by the deflection to the left of the GR log signature as a result of the fact that sand bodies will have a low concentration of radioactive minerals, while deflection to the right signified shale which is as a result of high concentration of radioactive minerals [33, 34]. Conventionally, the GR log is set to a scale of 0-150 API, with a central cut-off of 65 API units, in which less than 65 API is interpreted as sand, while greater than 65 API is interpreted as shale. Moreover, fluid determination involved analyzing sandstone units using the resistivity log, where high resistivity values suggested the presence of hydrocarbons and low values indicated brine. Furthermore, the distinction was based on the conductivity of brine compared to hydrocarbons [4,35-37].

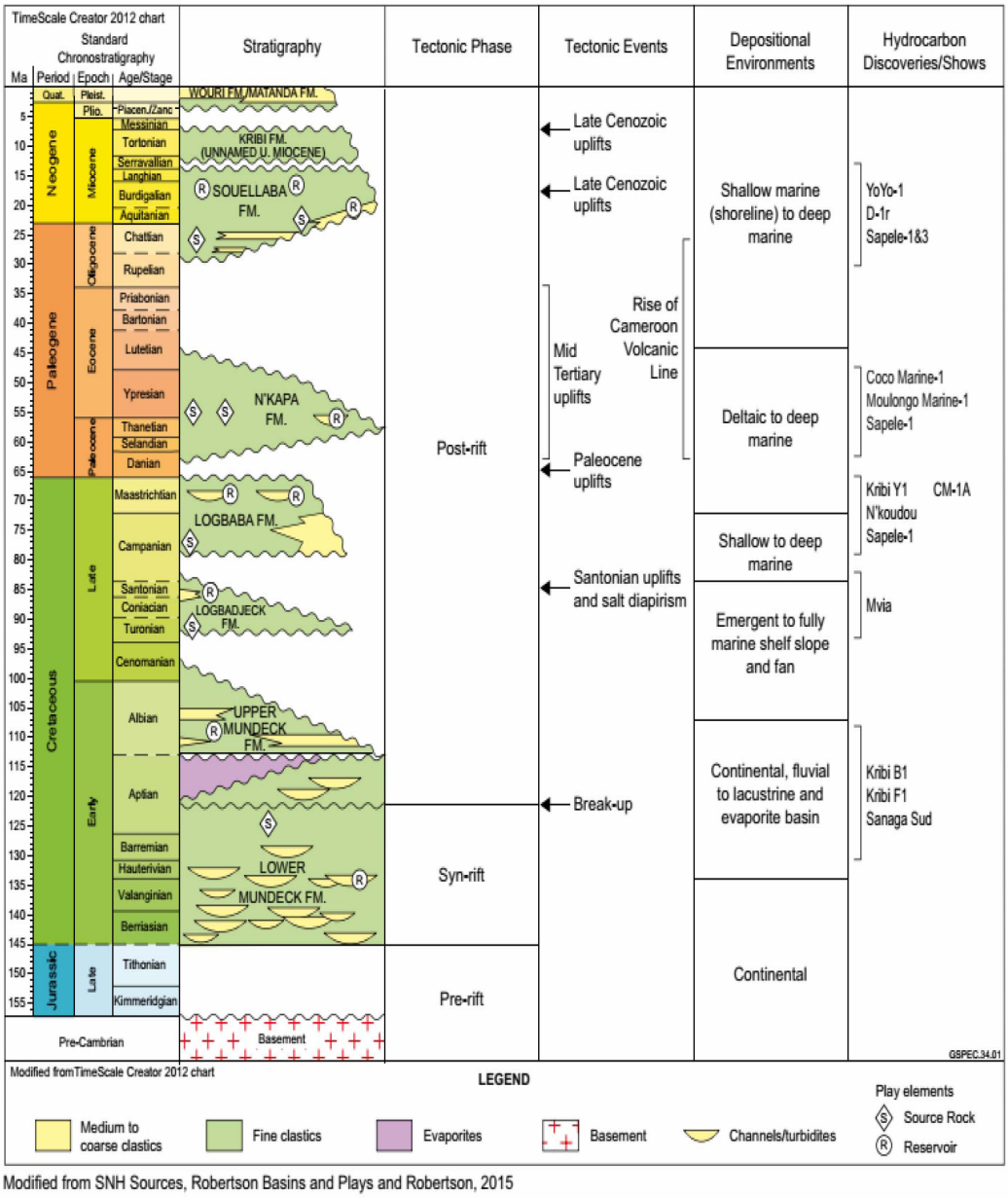

Modified from SNH Sources, Robertson Basins and Plays and Robertson, 2015

Fig. 3 Stratigraphic summary of the Douala/Kribi Campo basin indicating petroleum play [32].

The gamma ray log was utilized in the computation of shale volume within a porous reservoir. Initially, the gamma ray index was determined using Equation 1 to estimate shale volume; however, this method tends to overestimate the shale volume. To rectify this, the correction was made by applying [38] Equation 2.

Furthermore, the shale volume identified in the reservoirs through the gamma ray log was instrumental in adjusting both porosity and water saturation values. Moreover, the volume of shale (Vsh) indicates reservoir quality—the cleaner the reservoir is, the lower the shale volume is.

Porosity was assessed by inserting bulk density readings obtained from the density log into the [39] equation (i.e., Equation 3) within each reservoir. Additionally, total porosity was determined using Equation 4, and the interpretation of reservoir quality was facilitated by referring to the [40]. classification scheme.

$$I_{GR} = \frac{GR_{\log} - GR_{\min}}{GR_{\max} - GR_{\min}} \quad (1)$$

$$V_{sh} = 0.083[2^{(3.17 \times I)} GR] - 1.0 \quad (2)$$

NB: In Equation 1, IGR is the gamma ray index, GR log is the reading of formation, while GR minimum and GR maximum indicate values picked in the sand and shale base lines, respectively.

$$ØD = ρma - ρb / ρma - ρf \quad (3)$$

$$ØT = ØN + ØD/2 \quad (4)$$

where

ØD = density-derived porosity

ρma = matrix density (2.65gm/cm^3 (sandstone))

ρb = the formation bulk density

ρf = fluid density (1.1gm/cm^3)

ØT= Total porosity

ØN= Neutron porosity

The fluid saturation within a reservoir is usually expressed relative to the total pore space, where the fluids present could be saline water and/or hydrocarbons. The water saturation in the reservoir is contingent upon the amount of hydrocarbon present; a higher water saturation implies a

lower hydrocarbon content in the reservoir. Archie's saturation equation typically determines fluid saturation, but its efficacy can be limited in less clean sand formations. Subsequently, the water saturation in the reservoirs of this field was approximated using the Indonesian model (based on Equation 5) developed by [41]. which is tailored for shaly reservoirs like those encountered in this study.

$$W = \left\{ \left[\left(\frac{V_{sh}^{\,2-V_{sh}}}{R^{sh}} \right)^{\frac{1}{2}} + \left(\frac{\phi_e^m}{R^w} \right)^{\frac{1}{2}} \right]^2 R_t \right\}^{\frac{-1}{n}} \quad (5)$$

where;
V_{sh}: Volume of shale in reservoir,
R_w: Formation water resistivity at formation temperature,
R_t: True formation resistivity, n: Saturation exponent.
Hydrocarbon Saturation, Sh represents the hydrocarbon proportion within a formation's pore volume and was calculated by subtracting the water saturation value from 100%. Permeability was computed from log data utilizing the Tixier Equation 6.

$$k^{\frac{1}{2}} = \frac{250 \times \phi^3}{S_w irr} \quad (6)$$

where $S_w$irr is the irreducible water saturation
Reservoirs were graded based on their permeability levels, assisted by [41] permeability classification system. The Bulk Water Volume (BVW) in a reservoir is computed by multiplying the Water saturation (Sw) by the porosity (Ø) as expressed in Equation 7 below.

$$BVW = Sw\text{Ø} \quad (7)$$

Notably, BVW aids in indicating whether a reservoir is at Swirr, a state where it produces water-free hydrocarbons due to the retention of all the formation water through surface tension or capillary pressure by grains. Moreover, a reservoir at Swirr exhibits constant or nearly constant BVW values throughout, as elucidated by [2, 42]. Consequently, when BVW has been calculated at multiple points within an interval, the values should be comparable to signify an essentially water-free completion.
In order to obtain precise formation evaluation and assess the reservoir quality necessary for effective reservoir management, a thorough reservoir correlation was conducted between the wells within the field. This involved determining the deposition environment of the reservoir units in Well 1 and Well 2. Moreover, the correlation analysis of Well 1 and Well 2 was carried out by analyzing their respective well logs, which included gamma ray, resistivity, porosity, and lithology data. This analytical approach aids in identifying geological and reservoir characteristics by comparing the recorded log responses [43,44].
The beginning of this process involves selecting a representative reference well log for comparison with others through techniques such as cross-correlation and clustering. In addition, this correlation process assists in understanding the lateral continuity and variability of reservoir properties essential for tasks like well planning and reserve estimation [44].
The depositional environment of the reservoir units in Well 1 and Well 2 within the field was determined using the Self-potential and gamma ray log signatures in the absence of core samples as described by [45]. The distinct shapes of the curves can be attributed to factors such as water depth, the origin of sediment, and the prevailing hydrodynamic forces [46-49].

Results and Discussion

Results

Lithologic Sequence and Reservoir Unit

From the qualitative analysis of the well logs signature, three (3) sandy reservoirs were identified in Well 1 and Well 2 (Fig.4a-c). In addition, the lithologic sequences of Well 1 and Well 2 consist of sandstones beds alternating with shale (Fig.4a- c).

Fluid Type Present in the Reservoir

The fluid types identified in the reservoir units of Well 1 and Well 2 are formation water and hydrocarbon (Fig. 5a-c).
To determine the fluid composition within the reservoir units of Wells 1 and 2 and evaluate their viability for commercial hydrocarbon extraction, a plot was created. Moreover, this plot depicted the relationship between true formation resistivity (Rt) and water saturation (Sw) (Fig. 6 and Fig. 7). Furthermore, the findings from these plots indicate that the predominant fluid phase in the reservoir units (R1, R2, and R3) in both wells is mainly water, suggesting their incapacity to deliver a commercially viable quantity of hydrocarbons.

Petrophysical Properties

Table 4.1 offers a detailed overview of the petrophysical parameters calculated based on the examination of the well log data. The table showcases the diverse petrophysical parameters acquired through the analysis of well logs for the three (3) clastic reservoirs encountered by the corresponding individual wells.
The analysis of the permeability (k) and effective porosity (Φ) plot (Fig. 8 and Fig. 9) offered significant insights into the reservoir's physical attributes, including grain size, sorting, and cementation degree. Moreover, this plot facilitated the delineation of distinct zones indicating coarsening, fining, sorting, and cementation of clay within the reservoir. For well 1, the plot in Fig. 8 revealed that R1 is situated in a region characterized by fine grain size and poor sorting. At the same time, R2 and R3 are located in the cement clay zone, indicating poorly sorted sands with a medium grain size. In contrast, in well 2, reservoir unit R1 falls within the medium grain size field with better sorting compared to R2 and R3, which are positioned in the cement clay area and exhibit poor sorting (Fig. 9).

Reservoir Correlation

The analysis of reservoir correlation revealed a robust connection between Well 1 and Well 2, as evidenced by the gamma ray deflection (Fig.10). Both wells exhibited multiple clastic permeable units, within the reservoir units R1, R2, and R3. These formations displayed consistent log signatures and uniform thickness throughout the field, indicating comparable geological attributes. Furthermore, R1 and R2 demonstrated a thickness augmentation towards the east, while R3 exhibited a slight increase between the two wells (Fig.10).

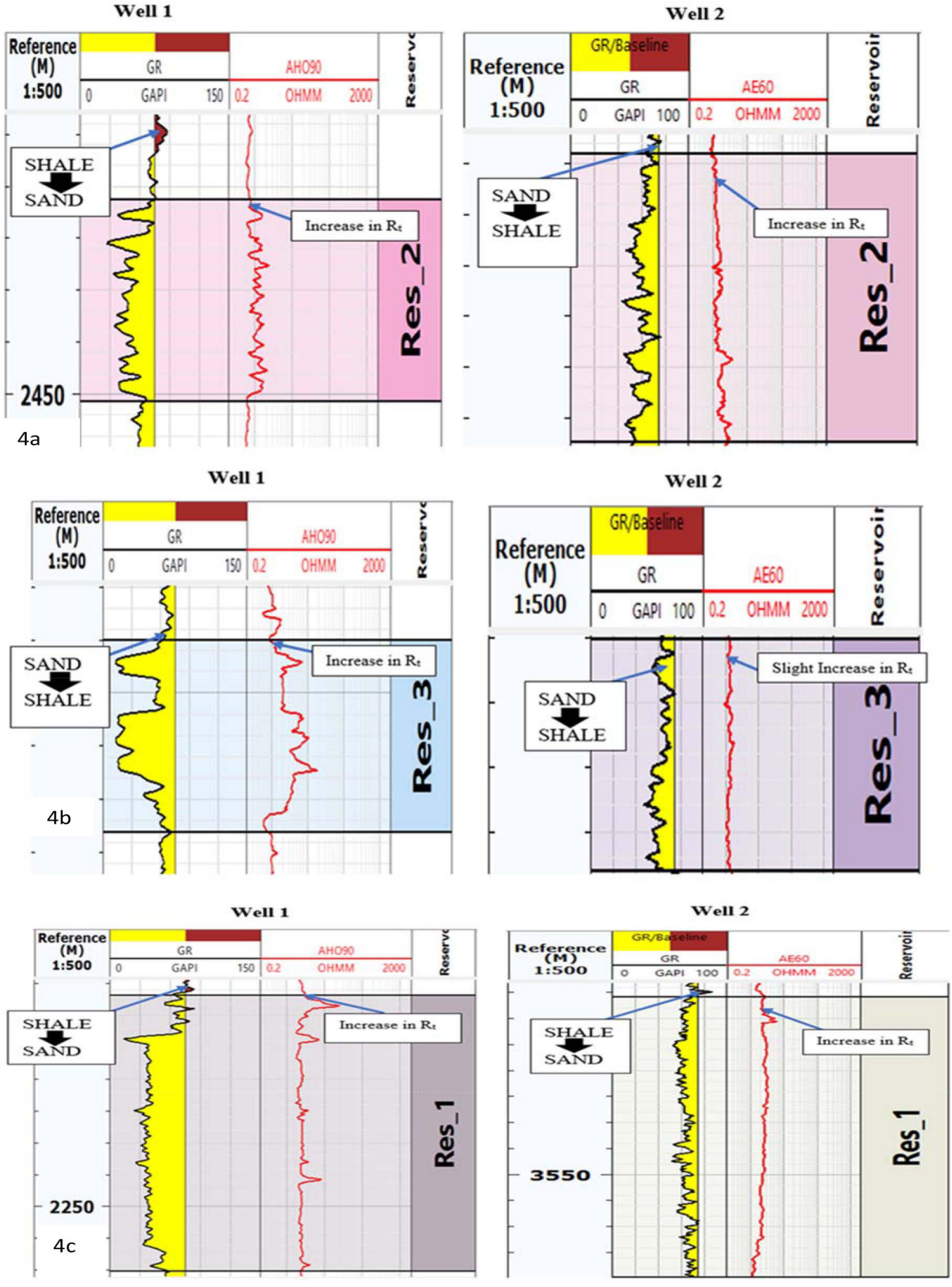

Fig. 4.a-c Log curves plot displaying sandstone reservoir interval three (R1, R2 & R3) using GR and Resistivity log signature of Well 1 and Well 2.

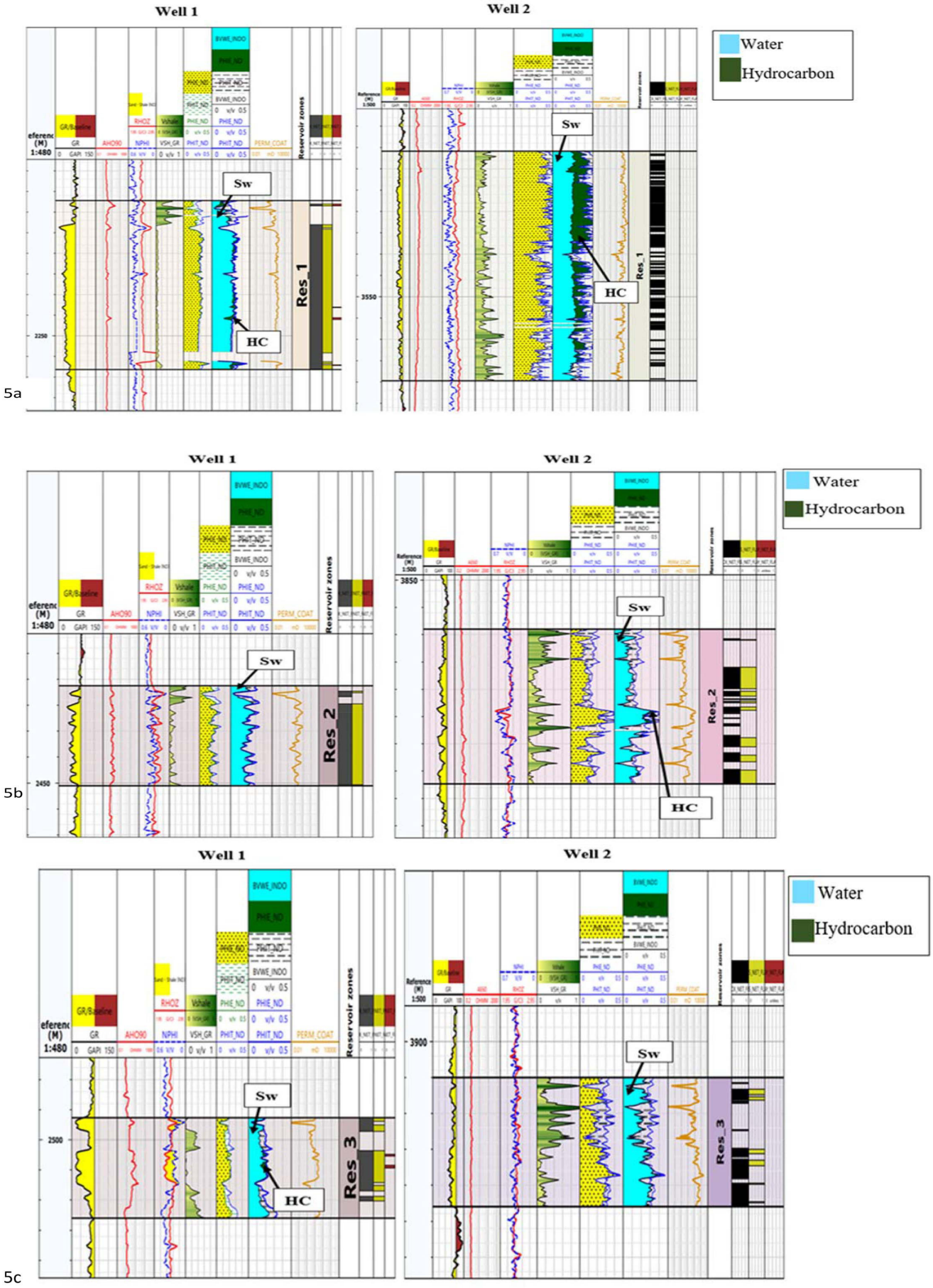

Fig. 5a-c Log curves plot displaying the fluid type identified from the reservoir units of Well 1 and Well 2.

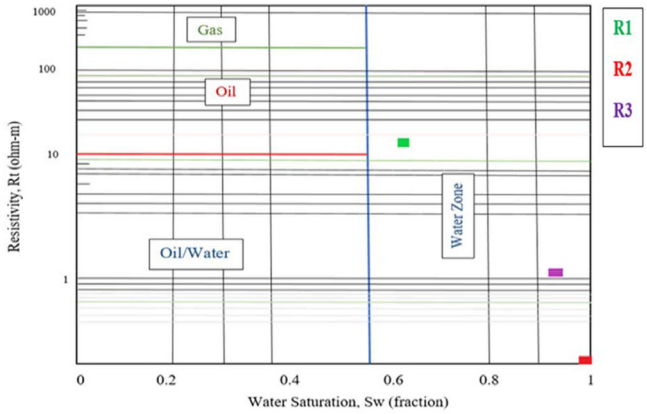

Fig. 6 Resistivity -Water Saturation cross plot of Well 1.

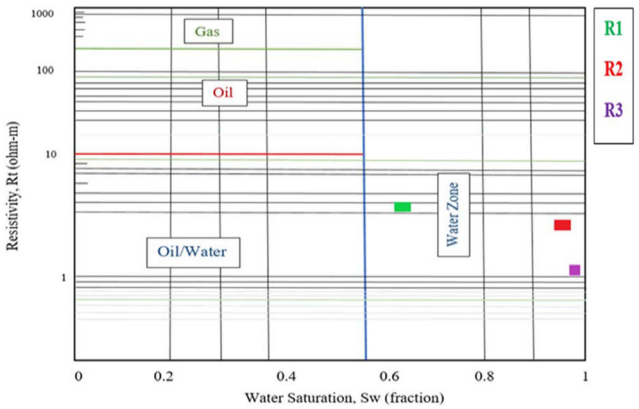

Fig. 7 Resistivity -Water Saturation cross plot of Well 2.

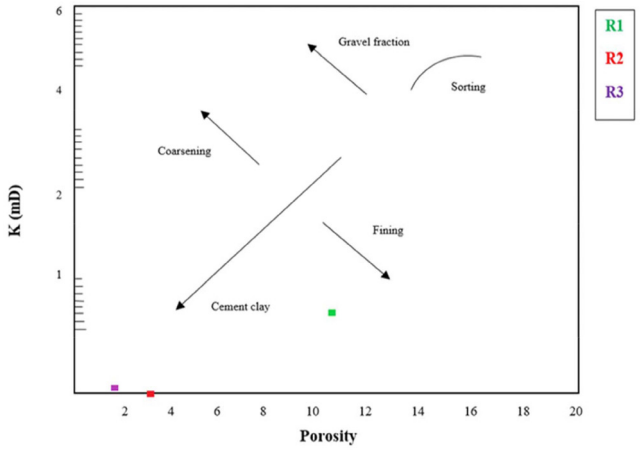

Fig. 8 Log Permeability vs. Porosity for Well 1.

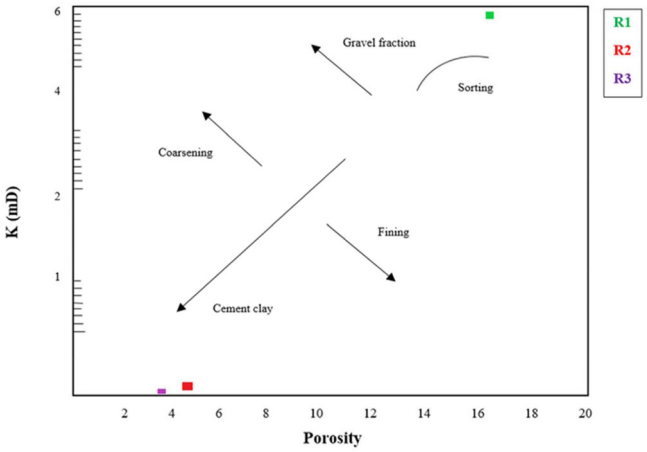

Fig. 9 Log Permeability vs. Porosity for Well 2.

Table 4 Petrophysical Parameters of the Reservoir Units in Well 1 and Well 2.

Reservoir 1									
	GROSS Thickness	NET PAY	N/G PAY	Phi(Φ)	Sw(%)	HC(%)	Vcl(v/v)	Perm (k)	BVW
WELL 1	40.99	1.219	0.03	9.115	65.51	34.49	0.058	0.508	8.684
WELL 2	53.84	30.328	0.563	16.534	64.1	35.9	0.166	5.933	10.601
AVERAGE	47.42	15.77	0.2965	12.8245	64.805	35.195	0.112	3.2205	9.6425
Reservoir 2									
	GROSS Thickness	NET PAY	N/G PAY	Phi (Φ)	Sw(%)	HC (%)	Vcl(v/v)	Perm(k)	BVW
WELL 1	19.261	0	0	3.203	100	0	0.069	0	3.242
WELL 2	28.31	13.912	0.5	4.8	98.2	1.8	0.342	0.084	4.679
AVERAGE	23.7855	6.956	0.25	4.0015	99.1	0.9	0.2055	0.042	3.9605
Reservoir 3									
	GROSS Thickness	NET PAY	N/G PAY	Phi (Φ)	Sw(%)	HC (%)	Vcl(v/v)	Perm (k)	BVW
WELL 1	16.658	0.762	0.046	1.537	92.40	7.60	0.046	0.053	1.416
WELL 2	18	9.296	0.516	3.911	99.5	0.5	0.123	0.02	3.911
AVERAGE	17.329	5.029	0.281	2.724	95.95	4.05	0.0845	0.0365	2.6635

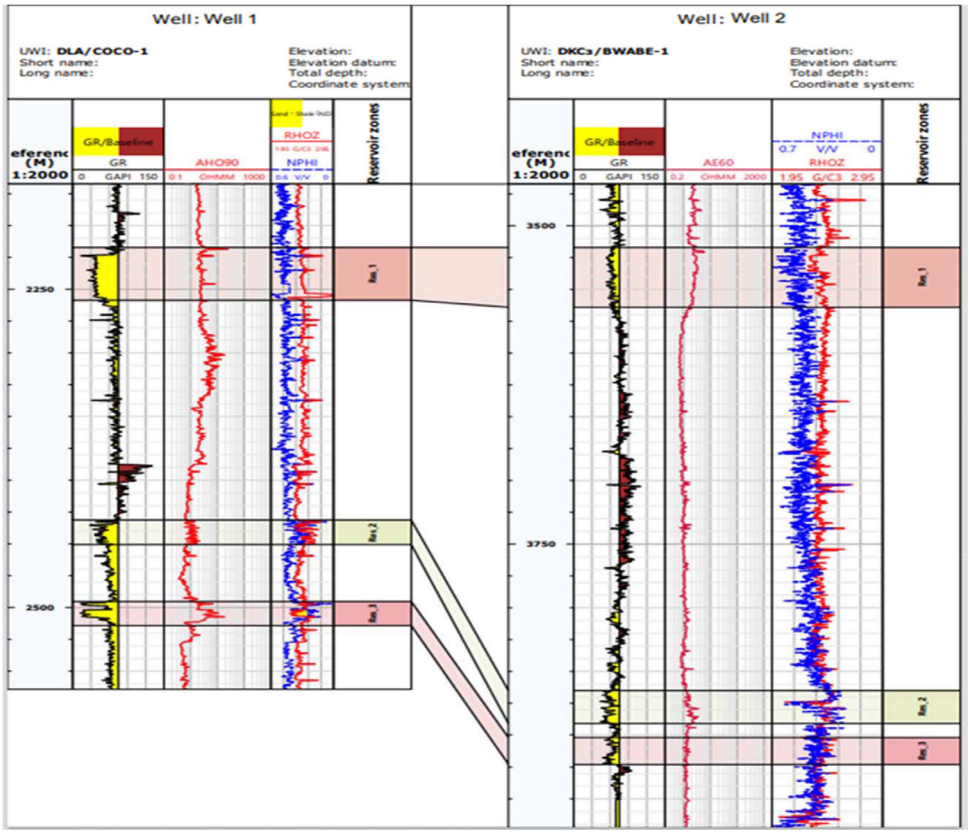

Fig. 10 Correlation panel of Well 1 and Well 2.

Depositional Environment

Analysis of the GR log patterns enabled the determination of the depositional environments of the reservoir units in Wells 1 and 2 [50]. In addition, the log characteristics in R1 of both wells offer valuable insights into the depositional mechanisms, revealing aggrading processes. Furthermore, in Well 1, the sand lithologies in R1 appear blocky and are identified as channel sands (Fig. 11). These deposits exhibit aggregational features, indicating distributary channel infill. Also, distributary channel sands are characterized by high energy and cleanliness, making them advantageous reservoirs with minimal shale content. In addition, conversely, the GR log motif of the sand unit in R1 in Well 2 displays a serrated pattern, suggesting a fluvial plain and a shelf environment dominated by storms (Fig.11).

In both wells, the GR log signatures of reservoir unit R2 demonstrate a diverse range of depositional environments, including fluvial floodplains, storm-dominated shelves, deep marine slopes, braided fluvial systems, and submarine canyons (Fig. 12).

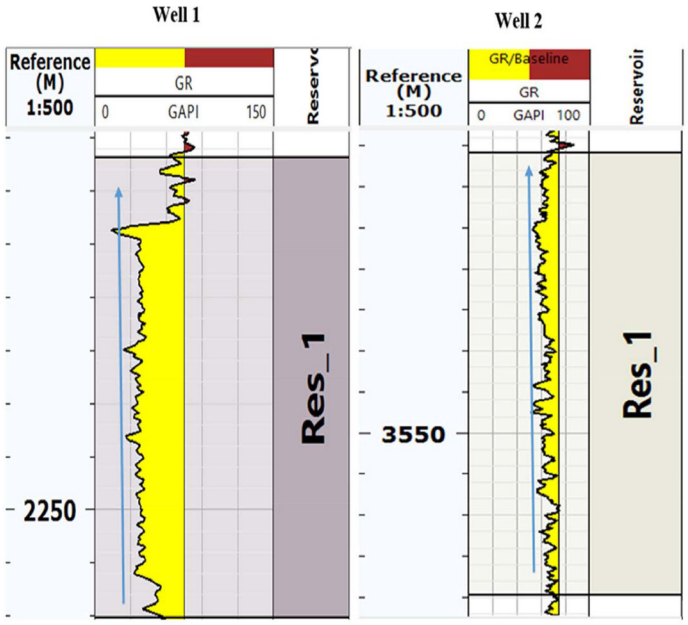

Fig. 11 Log motifs indicating depositional environment of reservoir unit R1 of Well 1 and Well 2.

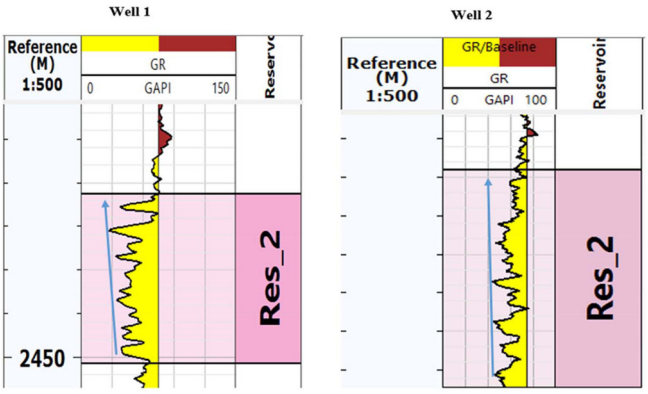

Fig. 12 Log motif indicating depositional environment of reservoir unit R3 of Well 1 and Well 2.

In reservoir unit R3 of well 1 and well 2, the log signatures suggest a funnel/bell shape (prograding/retrograding) as shown in Fig. 13. Moreover, this shape indicates that the depositional environment could include crevasse splay, river mouth bar, delta front, shore face, submarine fan lobe, transition from clastic to carbonate, fluvial point bar, tidal point bar, deep tidal channel fill, tidal flat, and transgressive flat, as defined by [51] Additionally, the gamma ray response and depositional setting described by [41] suggest deep-sea settings, specifically supra fan lobes.

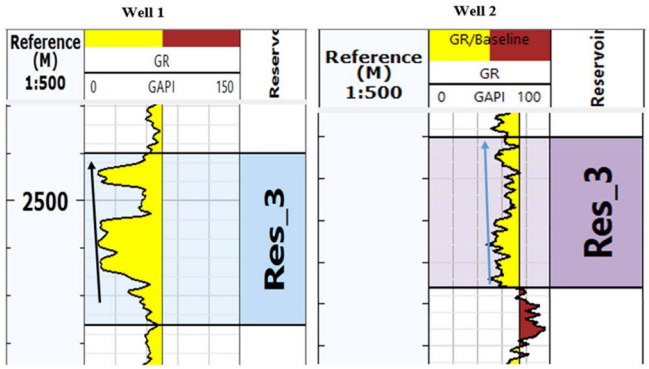

Fig. 13 Log motif indicating depositional environment of reservoir unit R3 of Well 1 and Well 2.

Discussion

The qualitative interpretation of gamma-ray (GR) logs from the studied offshore wells reveals a lithological composition predominantly comprising sandstones and shales. These findings are consistent with those of [52], who conducted a similar study in the Douala Basin aimed at identifying stratigraphic sequences. Their qualitative analysis of gamma-ray logs also revealed a characteristic lithologic pattern of sandstones and claystones. Similarly, [28] in their assessment of the petroleum potential of the Douala Basin, reported alternating layers of sandstone and shale, with sandstone units being more laterally extensive than shale in their study area. The reservoir units identified in the studied wells were deposited in various environments, including braided river floodplains, deep tidal channel fills, and submarine fan lobe sands. These environments exhibit aggrading, retrograding, and prograding processes, respectively. In addition, these observations are consistent with the findings of [53] in their study of the Douala basin, where they also identified channel sand, submarine fan lobe sands, and deep tidal channel fills as the depositional environments in their studied reservoirs. In their study, which focused on establishing the stratigraphic sequence and conducting facies analysis within the N'kapa formation, [54] identified progradational and retrogradational patterns indicative of floodplain and lacustrine deposits, fluvial/mouth bar deposits, and shoreface deposits. Additionally [53], in their examination of the N'kapa formation, highlighted a stratigraphic sequence through well log analysis, revealing reservoir deposition environments characterized by fluvial systems, deltaic plain facies, and tidal processes, which mirror the observations made in this research study. Across the studied wells, three reservoir units (R1, R2, and R3) were identified, showing a correlation between the wells. These reservoirs are associated with sand bodies, with average net pay thicknesses of 47.4 m, 23.8 m, and 17.3 m for R1, R2, and R3, respectively. Also, petrophysical analysis indicates poor reservoir quality for the identified reservoir units in Well 1 and Well 2. Ultimately, these findings contradict the observations made in the Douala basin by [24, 53] where the reservoirs in their study field displayed porosity of 20%, hydrocarbon saturation of 69%, and permeability of 76 mD.

Conclusions

This study has demonstrated that the three reservoir units (R1, R2, and R3) delineated are laterally continuous and correlate across both wells. Moreover, the lithological analysis of the GR logs reveals that the wells predominantly consist of thick sandstone layers with intermittent shale intercalations. Furthermore, petrophysical analysis indicates poor reservoir quality for the identified reservoir units in Well 1 and Well 2. Moreover, the GR log motif provides insights into the depositional environment of these sediments, suggesting that they were deposited in a deep marine environment, specifically fan valley sediments, which encompass braided river floodplains, deep tidal channel fills, and submarine fan lobes. Moreover, the evaluation of reservoir units in the AN Field in the Douala Basin highlights the presence of water-saturated reservoir units with poor petrophysical properties, indicating limited hydrocarbon potential.

Nomenclatures

Sw: Water saturation
GR: Gamma Ray

References

1. Helander, D. P. (1983). Fundamentals of formation evaluation. Oil & Gas Consultants International.
2. Asquith, G. B., Krygowski, D., & Gibson, C. R. (2004). Basic well log analysis (Vol. 16, pp. 305-371). Tulsa: American Association of Petroleum Geologists.
3. Obidike, C. C., & Chiazor, F. I. (2023). Petrophysical evaluation and depositional environments of reservoir sands in an oil producing field, Onshore Niger Delta, Nigeria. Journal of Applied Sciences and Environmental Management, 27(4), 639-645. doi:10.4314/jasem.v27i4.1.
4. Miall, A. D. (2018). Depositional environments. In R. Sorkhabi (Ed.), Encyclopedia of Petroleum Geoscience. (pp. 1–6). Springer. doi.org/10.1007/978-3-319-02330-

4_138-1.
5. Albeyati, F., Abdula, R., & Terzi, F. (2021). Porosity and permeability measurements integration of the Upper Cretaceous in Balad Field, Central Iraq. Iraqi Geological Journal, 54(1B), 24–42. https://doi.org/10.46717/igj.54.1B.3Ms-2021-02-21.
6. Aigbadon, G. O., Babatunde, G. O., Mu'awiya, B. A., Nanfa, C. A., & Christopher, S. D. (2021). Depositional environments and reservoir evaluation of otuma oil field, Niger-Delta basin, Nigeria. European Journal of Environment and Earth Sciences, 2(6), 53-57. doi:10.24018/ejgeo.2021.2.6.233.
7. Shanmugam, G., & Moiola, R. J. (1988). Types of submarine fan lobes: Models and implications. AAPG Bulletin, 75(1), 156–179. doi.org/10.1306/0C9B276D-1710-11D7-8645000102C1865D.
8. Journel, A. G. (1995). Geology and reservoir geology: Stochastic modeling and geostatistics. In J. M. Yarus & R. L. Chambers (Eds.), AAPG Computer Applications in Geology (pp. 19–20). AAPG.
9. Johnston, D. (2004). Reservoir characterization improves stimulation, completion practices. Oil & Gas Journal, 102(4), 60–63. ISSN 0030-1388 Scientific domain Energy.
10. Hilchie, D. W. (1990). Wireline: A history of the well logging and perforating business in the oil fields. DW Hilchie.
11. Schlumberger. (1977). Log interpretation charts. Schlumberger Well Services.
12. Uguru, C. I., Onyeagoro, O. U., & Sikiru, I. O. (2002). Permeability modeling for reservoirs in the Niger Delta based on geological descriptions and core data. SIPM Review Report, 4, 98.
13. Akpan, M. J., George, N. J., Ekanem, A. M., & Ekong, U. N. (2022). Petrophysical appraisal and 3D structural interpretation of reservoirs in an Onshore Niger Delta Field, Southeastern Nigeria. International Journal of Energy and Water Resources. doi.org/10.1007/s42108-022-00218-9.
14. Brownfield, M. E., & Charpentier, R. R. (2006). Geology and total petroleum systems of the Gulf of Guinea Province of West Africa (No. 2207-C). US Geological Survey.
15. Subrahmanyam, V., Krishna, K. S., Murthy, G. P. S., Rao, D. G., Ramana, M. V., & Rao, M. G. (1994). Structural interpretation of the Konkan basin, southwestern continental margin of India, based on magnetic and bathymetric data. Geo-marine letters, 14, 10-18.
16. Morley, C. K. (1995). Developments in the structural geology of rifts over the last decade and their impact on hydrocarbon exploration. Geological Society, London, Special Publications, 80(1), 1-32. doi.org/10.1144/gsl.sp.1995.080.01.01.
17. SNH – Société Nationale des Hydrocarbures. (2013). End-of-year report on prospect: The Douala/Kribi-Campo Basin.
18. Gazel, J. (1956). Carte géologique du Cameroun. Direction des Mines et de la Géologie du Cameroun.
19. Burke, K. (1972). Longshore drift, submarine canyons, and submarine fans in development of Niger Delta. AAPG bulletin, 56(10), 1975-1983. doi.org/10.1306/819A41A2-16C5-11D7-8645000102C1865D.
20. Ntamak-Nida, M. J., Bourquin, S., Makong, J. C., Baudin, F., Mpesse, J. E., Ngouem, C. I., Komguem, P.B. & Abolo, G. M. (2010). Sedimentology and sequence stratigraphy from outcrops of the Kribi-Campo sub-basin: Lower Mundeck Formation (Lower Cretaceous, southern Cameroon). Journal of African Earth Sciences, 58(1), 1-18. doi.org/10.1016/j.jafrearsci.2010.01.004.
21. Njoh, O. A. (2007). Upper Cretaceous Foraminiferal Biostratigraphic Correlations; Douala and Rio del Rey Basins (SW Cameroon) and Calabar Flank (SE Nigeria). Unpublished Doctoral Dissertation, University of Calabar, Nigeria.
22. Chongwain, G. M., Osinowo, O. O., Ntamak-Nida, M. J., & Nkoa, E. N. (2018). Seismic attribute analysis for reservoir description and characterization of M-Field, Douala Sub-Basin, Cameroon. Advances in Petroleum Exploration and Development, 15(1), 1–10. https://doi.org/10.3968/10220
23. Bekonga, B. S. G., Yem, M., Atangana, J. Q. Y., Nkoa Nkoa, P. E., Biouele, S. E. A., Niyazi, Y., & Eruteya, O. E. (2021). Seismic geomorphology of a Late Cretaceous submarine channel system in the Kribi/Campo sub-basin, offshore Cameroon. Marine and Petroleum Geology, 145, 105865. https://doi.org/10.1016/j.marpetgeo.2022.105865
24. Clotilde, O. A. M. L., Tabod, T. C., Séverin, N., Victor, K. J., & Pierre, T. K. A. (2013). Delineation of lineaments in South Cameroon (Central Africa) using gravity data. Open Journal of Geology, doi:10.4236/ojg.2013.35038.
25. SNH – Société Nationale des Hydrocarbures. (1999). Third licensing round: The Douala/Kribi-Campo Basin.
26. Kenfack, P. L., Ngaha, P. N., Ekodeck, G. E., Ngueutchoua, G., Kenfack, P. L., Ngaha, P. R. N., Ekodeck, G.E. & Ngueutchoua, G. (2012). Fossils dinoflagellates from the northern border of the Douala sedimentary sub-basin (South-West Cameroon): age assessment and paleoecological interpretations. Geosciences, 2(5), 117-124. doi: 10.5923/j.geo.20120205.03.
27. Minyem, D., & Nedelec, A. (1990). Origin and evolution of the Eseka gneisses (Cameroon): Archaean TTG rocks reworked in the Panafrican Mobile Belt. Publication occasionnelle-Centre international pour la formation et les échanges géologiques, (22), 21-24. ISSN 0769-0541.
28. Toteu, S. F., Penaye, J., & Djomani, Y. P. (2004). Geodynamic evolution of the Pan-African belt in central Africa with special reference to Cameroon. Canadian Journal of Earth Sciences, 41(1), 73-85. doi.org/10.1139/e03-079.
29. Ndikum, E. N., Tabod, C. T., Koumetio, F., Tatchum, N. C., & Victor, K. J. (2017). Evidence of some major structures underlying the Douala sedimentary sub-basin: West African Coastal Basin. Journal of Geoscience and Environment Protection, 5(7), 161-172. doi: 10.4236/gep.2017.57013.
30. Nguene, F. R., Tamfu, S., Loule, J. P., & Ngassa, C. (1992). Paleoenvironments of the douala and kribi/campo subbasins in Cameroon, West Africa. In Colloque de Géologie Africaine, Libreville (pp. 129–139).
31. Robertson. (2015). Exploration opportunities in two

producing basins in Cameroon. In Robertson Basins and Plays (Modified from SNH sources).
32. Hsieh, B.-Z., Lewis, C., & Lin, Z.-S. (2005). Lithology identification of aquifers from geophysical well logs and fuzzy logic analysis: Shui-Lin area, Taiwan. Computers & Geosciences, 31(3), 263–275. https://doi.org/10.1016/j.cageo.2004.07.004ResearchGate
33. Lai, J., Wang, G., Chen, M., Wang, S., Chai, Y., Cai, C., Zhang, Y., & Li, J. (2013). Evaluation of reservoir pore structure classification based on petrophysical phases: An example from the Long 8 oil formation in the Ji Plateau area of the Ordos Basin. Petroleum Exploration and Development, 40(5), 566–573. https://doi.org/10.11698/PED.2013.05.08.
34. Allen, G., & Unwin, L. (1983). Statistical methods in geology. George Allen & Unwin.
35. Wang, J. (2003). Use of a selected number of geo-genetic indicators with assessment of desertification in Tabernas–Sorbas area, Southern Spain. Unpublished IFA Report, ITC, Enschede, The Netherlands.
36. Avseth, P., Mukerji, T., & Mavko, G. (2005). Quantitative seismic interpretation: Applying rock physics tools to reduce interpretation risk. Cambridge University Press.
37. Stieber, S. J. (1970). Pulsed neutron capture log evaluation—Louisiana Gulf Coast. Paper presented at the Society of Petroleum Engineers Annual Fall Meeting, Houston, Texas. Society of Petroleum Engineers. https://doi.org/10.2118/2961-MS.
38. Dresser Atlas. (1979). Log interpretation charts. Dresser Industries.
39. Rider, M. (1986). The geological interpretation of well logs. Blackie.
40. Poupon, A., & Leveaux, J. A. C. Q. U. E. S. (1971, May). Evaluation of water saturation in shaly formations. In SPWLA Annual Logging Symposium (pp. SPWLA-1971). SPWLA.
41. Dewan, J. T. (1983). Modern open hole log interpretation. PennWell Publishing.
42. Lukeš, J. (2005). Methods of well logging used for borehole correlation in the granite stock, Podlesí granite, Bohemian Massif. Bull Geosci, 80(2), 155-161. ISSN 1214-1119.
43. Lüthi, S. (1981). Some new aspects of two-dimensional turbidity currents. Sedimentology, 28(1), 97-105. doi.org/10.1111/j.1365-3091.1981.tb01666.x.
44. Serra, O. (1986). Fundamentals of well-log interpretation: Vol. 2. The interpretation of logging data. Elsevier.
45. Selley, R. C. (1976). Subsurface Environmental Analysis of North Sea sediments. AAPG Bulletin, 60(2), 184-195. doi.org/10.1306/83D9229E-16C7-11D7-8645000102C1865D.
46. Selley, R. C. (1985). Elements of Petroleum Geology. W. H. Freeman.
47. Boggs, S. (1995). Principles of sedimentology and stratigraphy (2nd ed.). Prentice Hall.
48. Ellis, D. V., & Singer, J. M. (2007). Well logging for earth scientists (Vol. 692). Springer.
49. Kendall, C. (2003). Use of well logs for sequence stratigraphic interpretation of the subsurface. USC sequence stratigraphy web, University of South Carolina.
50. Emery, D., & Myers, K. J. (1996). Sequence stratigraphy. BlackwellScience.doi.org/10.1002/9781444313710
51. SPKN, L., BISSO, D., MM, E., & CO, M. (2023). High-resolution sequence stratigraphy from well-log patterns and base-level variations of the Paleocene-Early Eocene N'kapa Formation, Douala onshore Basin (SW Cameroon). doi.org/10.21203/rs.3.rs-3153670/v1
52. Chongwain, G. C., Osinowo, O. O., & Ntamak-Nida, M. J. (2019). Lithological typing, depositional environment, and reservoir quality characterization of the "M-Field," offshore Douala Basin, Cameroon. Journal of Petroleum Exploration and Production Technology, 9, 1705–1721. doi.org/10.1007/s13202-019-0669-z.
53. Kwetche Fowe, P. G., Ntamak-Nida, M. J., Djomeni Nitcheu, A., Etame, J., Owono, F., Mbesse, C., Kissaaka, J., Ngon Ngon, G. F., & Bilong, P. (2017). Facies analysis and sequence stratigraphy of Missole outcrops: N'Kapa Formation of the southeastern edge of Douala Sub-Basin (Cameroon). Earth Science Research, 7(1), 35–50. doi.org/10.5539/esr.v7n1p35.